JPEDAV (2009) 30:502–508
DOI: 10.1007/s11669-009-9574-2
1547-7037 ©ASM International

Phase Diagram and Thermodynamic and Transport Properties of the $DyBr_3$-LiBr Binary System

B. Kubikova, L. Rycerz, I. Chojnacka, and Marcelle Gaune-Escard

(Submitted April 3, 2009; in revised form May 29, 2009)

The phase diagram of the $DyBr_3$-LiBr binary system was derived from DSC measurements. It exhibits two eutectics and has two stoichiometric compounds. The first compound, Li_3DyBr_6, melts congruently at 803 K. The second one, Li_6DyBr_9 decomposes in the solid state at 656 K. The composition of the two eutectic mixtures, $x(DyBr_3) = 0.156$ and 0.321, respectively, was determined by the Tamman method. The respective eutectic temperatures are 787 and 791 K. The electrical conductivity of Li_3DyBr_6 compound was measured in the liquid and solid phase. It was found to be a solid electrolyte with a high electrical conductivity at around room temperature. Some additional electrical conductivity measurements performed on solid samples confirmed the existence of Li_6DyBr_9.

Keywords enthalpy, phase diagram, rare earth alloys and compounds, thermal analysis, thermodynamic properties

1. Introduction

Despite two hundred years of lanthanide history, the thermodynamic data on their halide systems available in literature are scarce and it is not uncommon that the values appearing in reference tables come from estimation. In addition, experimental data in literature are very often contradictory. All the binary lanthanide-alkali metal chloride systems have been examined at large by Seifert.[1] However, the phase diagrams of the homologous bromide and iodide systems have not been fully investigated nor critically assessed yet. Among the little information available, some lanthanide-alkali metal bromide systems seem totally erroneous: the $TmBr_3$-RbBr system[2] for instance has surprisingly no congruently melting compound been reported, which is inconsistent with the general trends observed for all the LnX_3-RbX systems already characterized. Other systems were investigated,[3] but resulted in mostly graphic-only information. Therefore, more details would be required to fully characterize those systems. The above discrepancies or lack of data, of the many LiBr-$LnBr_3$ binary systems call for further investigations into lanthanide bromide-based systems. We therefore, decided to tackle this goal as a logical continuation of our large program focussed on the thermodynamics, structure and electrical conductivity of lanthanide halides and lanthanide-alkali metal halide systems.

The present article reports the phase diagram of the $DyBr_3$-LiBr binary system which includes in particular the Li_3DyBr_6 compound. Specific investigations were conducted on this compound; its electrical conductivity revealed solid electrolyte properties.

2. Experimental

2.1 Chemicals

Dysprosium(III) bromide was synthesized from the dysprosium oxide, Dy_2O_3. This oxide was dissolved in hot concentrated HBr acid. The solution was evaporated and $DyBr_3 \cdot xH_2O$ was crystallized. Ammonium bromide was then added and this wet mixture of hydrated $DyBr_3$ and NH_4Br was slowly heated first up to 450 and then up to 570 K to remove the water. The resulting mixture was subsequently heated to 650 K for sublimation of NH_4Br. Finally, the salt was melted at about 1250 K. Crude $DyBr_3$ was purified by distillation under reduced pressure (~0.1 Pa) in a quartz ampoule at 1250 K. $DyBr_3$ prepared in this way was of a high purity—min. 99.9%. Chemical analysis was performed by mercurimetric (bromine) and complexometric (dysprosium) methods. The results were as follows: Dy, $40.35 \pm 0.08\%$ (40.40% theoretical); Br, $59.65 \pm 0.11\%$ (59.60% theoretical).

Lithium bromide (LiBr) was Merck Suprapur reagent (minimum 99.9%). Before use, it was progressively heated

This article is an invited paper selected from participants of the 14th National Conference and Multilateral Symposium on Phase Diagrams and Materials Design in honor of Prof. Zhanpeng Jin's 70th birthday, held November 3-5, 2008, in Changsha, China. The conference was organized by the Phase Diagrams Committee of the Chinese Physical Society with Drs. Huashan Liu and Libin Liu as the key organizers. Publication in *Journal of Phase Equilibria and Diffusion* was organized by J.-C. Zhao, The Ohio State University; Yong Du, Central South University; and Qing Chen, Thermo-Calc Software AB.

B. Kubikova, Institute of Inorganic Chemistry SAS, Dúbravská cesta 9, 845 36 Bratislava, Slovakia; **L. Rycerz** and **I. Chojnacka**, Chemical Metallurgy Group, Faculty of Chemistry, Wroclaw University of Technology, Wybrzeze Wyspianskiego 27, 50-370 Wroclaw, Poland; **Marcelle Gaune-Escard**, Ecole Polytechnique, IUSTI CNRS UMR 6595, Technopole de Chateau-Gombert, 5 rue Enrico Fermi, 13453 Marseille Cedex 13, France. Contact e-mails: Marcelle.Gaune-Escard@polytech.univ-mrs.fr and Molten.Salts@polytech.univ-mrs.fr.

up to fusion under gaseous HBr atmosphere. Excess of HBr was then removed from the melt by argon bubbling. All chemicals were handled inside a high purity argon atmosphere in a glove box (water content <2 ppm).

2.2 Measurements

The appropriate amounts of $DyBr_3$ and LiBr were melted in vacuum-sealed quartz ampoules. The melts were homogenized and solidified. These samples were ground in an agate mortar in a glove box. Homogenous mixtures of different compositions were prepared in this way and used in phase diagram measurements. Although only about 5 g of Li_3DyBr_6 compound were necessary for electrical conductivity measurements, about 25 g of it were synthesized in order to avoid deviation from stoichiometry.

Setaram DSC 121 differential scanning calorimeter (DSC) was used to investigate phase equilibrium in the $DyBr_3$-LiBr system. Experimental samples (300-500 mg) were contained in vacuum-sealed quartz ampoules. Experiments were conducted at heating and cooling rates ranging 0.1-5 K min^{-1}. Because of the temperature limitation of DSC 121 (1100 K), liquidus temperatures of mixtures rich in $DyBr_3$ were determined using a Paulik-Erdey thermal analyzer. Liquidus temperatures were determined as temperatures corresponding to the related peaks maximum. In all other cases onset temperature (T_{ons}) was determined as effect temperature.

Heat capacity was measured with the same Setaram DSC 121 operated in a stepwise mode. This so-called "step method," has been described[4-6] previously. The same operating conditions (i.e., initial and final temperatures, temperature increment, isothermal delay, and heating rate) were used in all experimental series. Experimental monitoring, data acquisition, and processing were performed with the Setaram Setsys software. In the present heat capacity experiments, each 10 K heating step was followed by a 400-s isothermal delay. The heating rate was 1.5 K min^{-1}. The mass difference of the quartz cells in any individual experiment did not exceed 1 mg (cell mass: 400-500 mg).

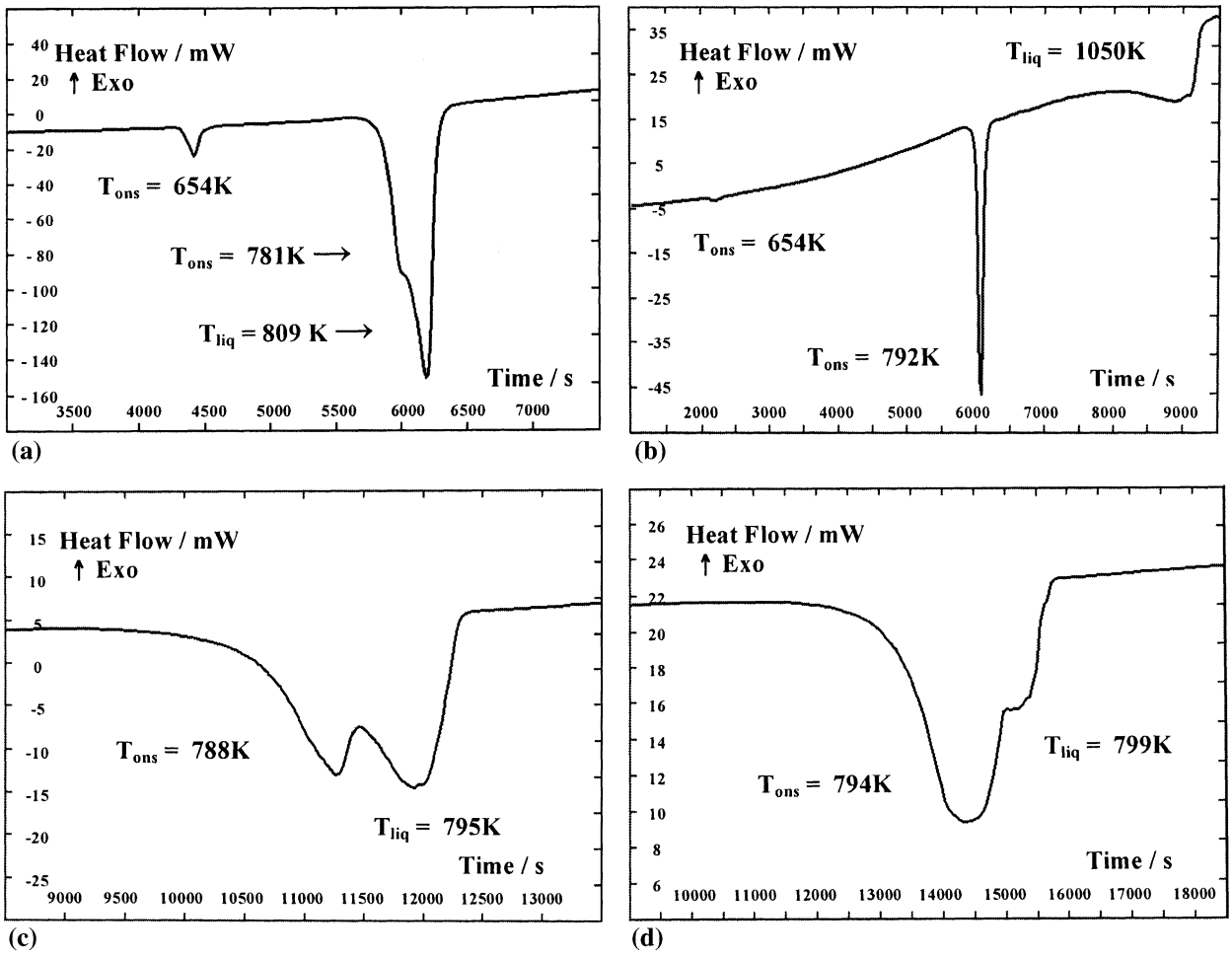

Fig. 1 DSC heating thermograms for $DyBr_3$-LiBr mixtures of different composition x and at various heating rate: (a) $x = 0.049$, heating rate = 5 K min^{-1}; (b) $x = 0.696$, heating rate = 5 K min^{-1}; (c) $x = 0.228$, heating rate = 0.1 K min^{-1}; (d) $x = 0.299$, heating rate = 0.1 K min^{-1}

Electrical conductivity measurements were carried out in a capillary quartz cell described in details elsewhere,[7] and calibrated with molten NaCl.[8] The conductivity of the melt was measured by platinum electrodes with the conductivity meter Tacussel CD 810 during increasing and decreasing temperature runs. The mean values of these two runs were used in calculations. Experimental runs were performed at a heating and cooling rate of 1 K min^{-1}. Temperature was measured with a Pt/Pt-Rh(10) thermocouple with 1 K accuracy. Temperature and conductivity data acquisition was made with PC computer interfaced to the conductivity meter. All measurements were carried out under static argon atmosphere. The accuracy of measurements was estimated at ±2%.

3. Results

3.1 Phase Diagrams

DSC investigations performed on samples with different compositions yielded both the temperature and the fusion enthalpy of the concerned mixtures. Due to supercooling effect, all temperature and enthalpy values reported here were determined from heating curves.

Figure 1(a) and (b) shows the thermograms for samples with molar fraction of $DyBr_3$, $x = 0.049$ and 0.696, respectively, obtained with a heating rate of 5 K min^{-1}.

In the composition range $0 < x < 0.250$ three endothermic peaks were present in all heating thermograms. The third effect, occurred at the highest temperature, can undoubtedly be ascribed to the liquidus temperature. The second one, at 787 K (mean value for all samples), is observable in all thermograms up to $x = 0.250$, where it disappears; thus suggesting the existence of a compound with the stoichiometry Li_3DyBr_6. Indeed, only a single thermal effect was observed in all samples of this composition $x = 0.250$, which was assigned to the congruent fusion of this compound at 803 K.

The existence of the Li_3DyBr_6 compound has already been mentioned and its crystal structure has been described.[9] Therefore, it is obvious that the second thermal effect at 787 K corresponds to the LiBr-Li_3DyBr_6 eutectic. The eutectic and liquidus temperatures are very close altogether, and the corresponding thermal effects overlap. It was difficult to determine the enthalpy of the eutectic melting even at very slow heating rate (0.1 K min^{-1}). Therefore, a semi-quantitative procedure was applied to deconvoluate these overlapping peaks in thermograms (Fig. 1c, d). Total enthalpy related to these two effects, which is proportional to the surface, was obtained from thermograms. Subsequently the heights of peaks were determined. Assuming that the height of the peak is proportional to its surface it was possible to determine the ratio of the surfaces, and thus the enthalpy related to the effect corresponding to the eutectic.

The eutectic contribution to the enthalpy of fusion is plotted against composition in Fig. 2, curve (A). This so-called Tamman construction makes it possible to evaluate the eutectic composition from the intercept of the two linear parts in Fig. 2, curve (A), as $x = 0.156$. The eutectic mixture melts with the enthalpy, $\Delta_{fus}H_m$, of about 12.4 kJ mol^{-1}. In this Tamman construction it was assumed that there was no solubility in the solid state. Thus, the straight lines intercept the composition axis at $x = 0.0$ and $x = 0.250$.

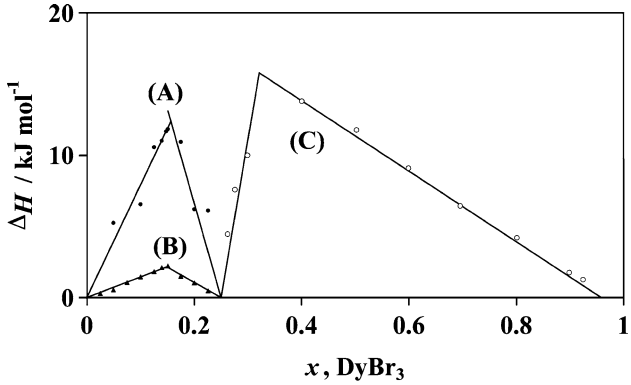

Fig. 2 Tamman diagrams for the $DyBr_3$-LiBr system: (A) black circles—determination of LiBr-Li_3DyBr_6 eutectic composition, (B) black triangles—stoichiometry determination of compound that decomposes in the solid state, (C) open circles—determination of Li_3DyBr_6-$DyBr_3$ eutectic composition

In the thermograms corresponding to samples in the composition range $0 < x < 0.250$, the first thermal effect occurs at 656 K (mean value from all appropriate thermograms). A similar construction, i.e., enthalpy versus composition (Fig. 2, curve (B)) suggested that another compound exists in this composition range and yielded $x = 0.149$ for its composition. This corresponds to the stoichiometry Li_6DyBr_9 (theoretical value $x = 0.143$). Thus, this thermal effect can be attributed to the decomposition of this compound in the solid state.

In the composition range $0.250 < x < 1$, DSC experiments resulted in thermograms with two endothermic peaks followed by a third and final thermal event at the liquidus temperature (Fig. 1b). The first effect at 475 K is related to dysprosium bromide, as it appears also in pure $DyBr_3$. However, its nature is unknown. Only a rhombohedral $FeCl_3$-type crystal structure and no solid-solid transition have been reported for $DyBr_3$.[10] However, we did observe a small endothermic effect at 488 K in pure $DyBr_3$. It should be pointed out that this effect was observable on all samples prepared from different batches and tested for purity by chemical analysis. A tentative explanation could be the existence of an unknown stable or metastable phase, which could transform at 488 K. This hypothesis is suggested by the similar behavior observed previously in $DyCl_3$.[11] Indeed, we have identified[11] a solid-solid phase transition in $DyCl_3$ at 611 K with an enthalpy change, $\Delta_{trs}H_m$, of about 1.4 kJ mol^{-1}. This transition had not been reported in literature, probably from the monoclinic, $AlCl_3$-type, to the orthorhombic, $PuBr_3$-type, structure. However, we have pointed out that information concerning the crystal

structure of $DyCl_3$ was and still is unclear. Templeton and Carter[12] claimed that only one allotropic variety of $DyCl_3$ exists, i.e., monoclinic, $AlCl_3$-type, whereas Bommer and Hohman[13] argued for two modifications: namely the monoclinic, $AlCl_3$-type and the orthorhombic, $PuBr_3$-type. Weigel and Wishnewsky[14] found that the monoclinic, $AlCl_3$-type structure of $DyCl_3$ transforms at 790 K under high pressure into an orthorhombic, $PuBr_3$-type structure.

The second endothermic effect at 791 K in the composition range $0.250 < x < 1$ is related to the Li_3DyBr_6-$DyBr_3$ eutectic. The enthalpy change corresponding to this effect was plotted against composition in Fig. 2, curve (C). The eutectic composition was determined from the intercept of the two linear parts in this figure as $x = 0.321$. The melting enthalpy, $\Delta_{fus}H_m$, related to this eutectic mixture is about 15.8 kJ mol^{-1}. This Tamman construction also gives information about the formation of solid solutions in the $DyBr_3$-rich side since the straight line obtained for mixtures beyond the eutectic composition did not intercept the composition axis at $x = 1$. The molar fractions at which solid solutions may exist at 791 K were found (Fig. 2, curve (C)) as $x \geq 0.958 \pm 0.005$. The complete phase diagram is presented in Fig. 3.

3.2 Electrical Conductivity and Heat Capacity of Li_3DyBr_6 Compound

Impedance spectroscopy and ^{7}Li-NMR spectroscopy investigations[9] showed that the Li_3DyBr_6 compound has a monoclinic (*C2/m*) crystal structure with highly mobile lithium ions.

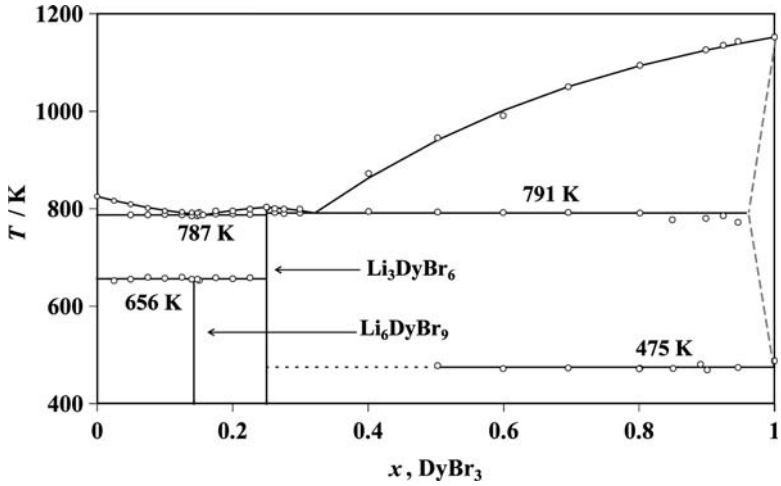

Fig. 3 Phase diagram of the $DyBr_3$-LiBr binary system

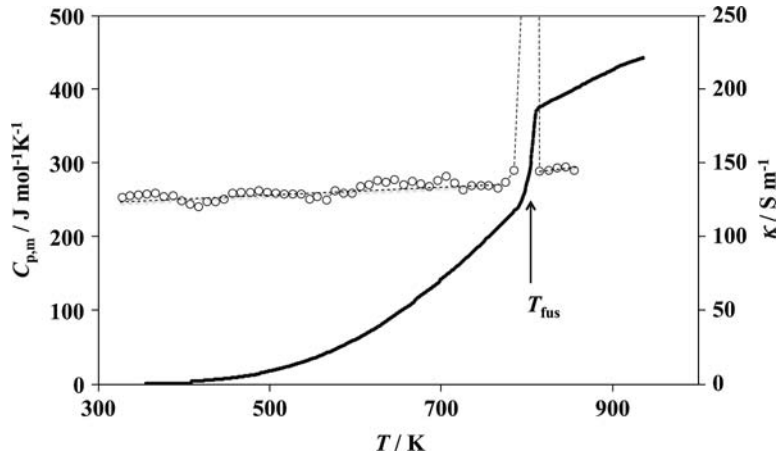

Fig. 4 Electrical conductivity and heat capacity of Li_3DyBr_6: circles and dashed line—experimental heat capacity and linear fitting, respectively, solid line—electrical conductivity

Table 1 Least square regression analysis of electrical conductivity data for Li_3DyBr_6

Temp. range, K	ln κ_0, S m^{-1}	E_A, kJ mol^{-1}	ln s, S m^{-1}
360-486	8.1298	25.3 ± 0.1	0.0318
487-789	9.3659	29.7 ± 0.1	0.0181

Such a high mobility might come from crystal lattice defect formation. If so, this should be reflected both in electrical conductivity and heat capacity of the solid phase. Thus, we decided to measure the electrical conductivity and heat capacity of the Li_3DyBr_6 compound over a wide temperature range with a special focus on the solid state.

Indeed, Li_3DyBr_6 has a very high ionic conductivity even around room temperature. In the experimental temperature range, its electrical conductivity increases quickly with temperature from 0.75 S m^{-1} at 355 K, to 3.89 S m^{-1} at 450 K, 30.46 S m^{-1} at 600 K, and up to 114.98 S m^{-1} at 780 K (Fig. 4). The Arrhenius equation:

$$\kappa = \kappa_0 \cdot \exp\left(\frac{-E_A}{RT}\right) \qquad \text{(Eq 1)}$$

was fitted to the experimental results, in the temperature range where the dependence $\ln\kappa = f(T^{-1})$ could be approximated with a linear function. The pre-exponential factor κ_0 (S m^{-1}) and activation energy E_A (kJ mol^{-1}) were calculated by the least squares method. All these parameters and standard error of estimation s are shown in Table 1.

The Arrhenius plot $\ln\kappa = f(T^{-1})$ in Fig. 5, is indicative of the complex transport process in this compound. It consists of two linear parts, with a jump in $\ln\kappa$ at about 486 K, indicating two conductivity regimes in solid Li_3DyBr_6. The related activation energies, $E_A = 25.3 \pm 0.1$ kJ mol^{-1} and $E_A = 29.7 \pm 0.1$ kJ mol^{-1}, were obtained in the temperature ranges 360-486 K and 487-789 K, respectively.

The electrical conductivity of solid Li_3DyBr_6 has been measured by impedance spectroscopy[9] with experimental data only reported in graphical form. A simple visual comparison of that plot with Fig. 5 of the present work indicates large discrepancy: far larger electrical conductivity values were obtained in the present work. The only numerical value given in Bohnsak et al.,[9] 1 S m^{-1} at 573 K, is considerably lower than ours at the same temperature (29 S m^{-1}). Even if two regimes for conductivity have been also observed by the previous authors, breaking at 500 K, significantly larger activation energies for these regimes (70.5 and 125 kJ mol^{-1}) have been obtained. Concerned with the large differences observed, we repeated experimental runs under various conditions (several conductivity cells with different cell constants, several compounds from different synthesis batches) but found reproducibly and consistently the same conductivity values. At the present time, we are unable to give any explanation for these discrepancies.

Very often, a large conductivity increase in ionic solids results from the formation of defects.[15-17] The most commonly used experimental methods for testing disorder models and for quantitatively determining disorder data are conductivity, diffusion measurements and heat capacity measurements. An increase in the intrinsic disorder in the crystal lattice with temperature would require more energy, and this in turn increases the heat content of the crystal. The specific heat must therefore contain a component due to the change in disorder with temperature. Indeed, we have observed this phenomenon in silver chloride and bromide.[18] Disordering of the cationic sublattice was related to a significant and simultaneous increase of both electrical conductivity and heat capacity.

Therefore, under the hypothesis that the very high electrical conductivity increase in Li_3DyBr_6 was related to disordering in the crystal lattice, we were anticipating an increase in heat capacity.

Surprisingly, no rapid rise in heat capacity (which could be related to an increase in disorder) could be observed in preliminary heat capacity measurements (Fig. 4). This suggests that even at temperatures close to ambient, some kind of disorder, probably connected with cationic sublattice, must already be present. This conclusion is in good agreement with literature information. According to Bohnsak et al.,[9] the Li_3DyBr_6 compound has the monoclinic (*C2/m*) crystal structure. Impedance spectroscopy and ^{7}Li-NMR spectroscopy showed that the lithium ions in this structure are highly mobile.[9]

Electrical conductivity measurements of solid Li_3DyBr_6 and LiBr-$DyBr_3$ mixtures with molar fraction of $DyBr_3$, $x = 0.095$ and $x = 0.177$ (Fig. 6) also confirmed existence of Li_6DyBr_9 compound, which decomposes in the solid state at 656 K. Electrical conductivity of a composition $x = 0.177$, which is a mixture of Li_3DyBr_6 and Li_6DyBr_9 below 658 K is clearly smaller than pure Li_3DyBr_6. It indicates that Li_6DyBr_9 is not a solid electrolyte. However, the Li_3DyBr_6 part in the mixture still results in a high conductivity.

In the mixture with $x = 0.095$ electrical conductivity is very small up to about 660 K. This mixture contains only LiBr and Li_6DyBr_9 at <660 K, both with low conductivities. After Li_6DyBr_9 decomposition at 656 K into LiBr and Li_3DyBr_6, the electrolyte phase Li_3DyBr_6 appears and electrical conductivity increases significantly with temperature.

Acknowledgments

Financial support by the Polish Ministry of Science and Higher Education from budget on science in 2007-2010 under the Grant No. N204 4098 33 is gratefully acknowledged. B.K., L.R., and I.Ch. wish to thank the Ecole Polytechnique de Marseille for hospitality and support during this work.

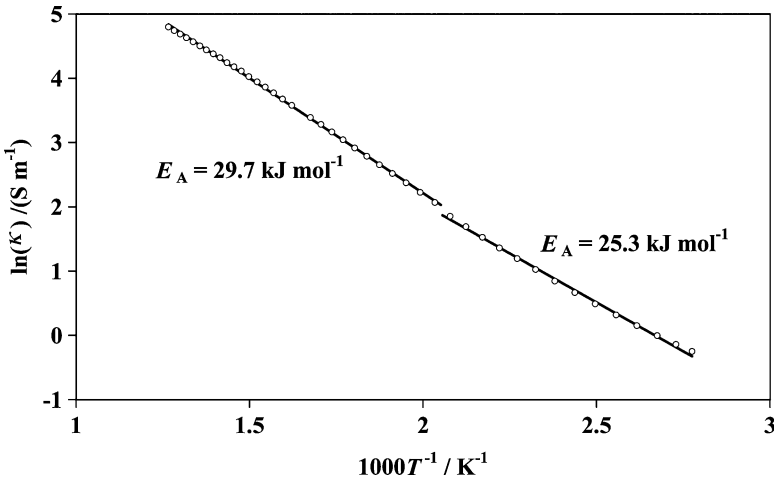

Fig. 5 Plot of ln(κ) vs. 1000/*T* for Li_3DyBr_6 in temperature range 360-789 K (for figure clarity only selected points with step 10 K are presented)

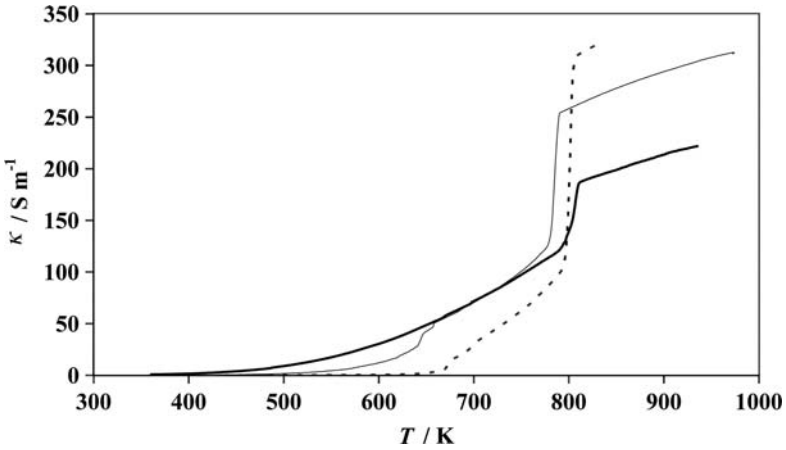

Fig. 6 Electrical conductivity of Li_3DyBr_6 (thick solid line) and LiBr-$DyBr_3$ mixtures with molar fraction of $DyBr_3$, $x = 0.177$ (thin solid line) and $x = 0.095$ (broken line)

References

1. H.J. Seifert, Ternary Chlorides of the Trivalent Late Lanthanides, *J. Thermal Anal. Calor.*, 2006, **83**(2), p 479-505, and references therein
2. A.K. Molodkin, A.M. Karagodina, A.G. Dudareva, and A.B. Strekachinskii, $TmBr_3$-RbBr System, *Zh. Neorg. Khim.*, 1981, **26**(8), p 2265-2267, in Russian
3. R. Blachnik and A. Jaeger-Kasper, Phase Diagrams of Alkali Bromide-Lanthanoid (III) Bromide Mixtures, *Z. Anorg. Allg. Chem.*, 1980, **461**, p 74-86
4. L. Rycerz, *High Temperature Characterization of LnX_3 and LnX_3-AX Solid and Liquid Systems (Ln = Lanthanide, A = Alkali, X = Halide): Thermodynamics and Electrical Conductivity*, Ph.D. Thesis, Marseille, 2003
5. L. Rycerz, *Thermochemistry of Lanthanide Halides and Compounds Formed in Lanthanide Halide-Alkali Metal Halide Systems*, (in Polish), Scientific Papers of Institute of Inorganic Chemistry and Metallurgy of Rare Elements, Wroclaw University of Technology, Series Monographs 35, Wroclaw, 2004
6. L. Rycerz, E. Ingier-Stocka, M. Berkani, and M. Gaune-Escard, Thermodynamic Functions of Congruently Melting Compounds Formed in $CeBr_3$-KBr Binary Systems, *J. Chem. Eng. Data*, 2007, **52**(4), p 1209-1212
7. Y. Fouque, M. Gaune-Escard, W. Szczepaniak, and A. Bogacz, Synthèse, Mesures des Conductibilités Electriques et des Entropies de Changements d'état Pour le Composé Na_2UBr_6, *J. Chim. Phys.*, 1978, **75**(4), p 360-366
8. G.J. Janz, High Temperature Calibration Quality Data: Molten Salts and Metals, *Mater. Sci. Forum*, 1991, **73-75**, p 707-714
9. A. Bohnsak, G. Balzer, M.S. Wickleder, H.U. Gudel, and G. Meyer, Ternary Halides of the A_3MX_6Type. VII. The Bromides Li_3MBr_6 (M = Sm, Lu, Y): Synthesis, Crystal

Structure, and Ionic Mobility, *Z. Anorg. Allg. Chem.*, 1997, **623**, p 1352-1356
10. C.P. Groen, E.H.P. Cordfunke, and M.E. Huntelaar, The Thermodynamic Properties of $DyBr_3$(s) and DyI_3(s) from T = 5 K to Their Melting Temperatures, *J. Chem. Thermodyn.*, 2003, **35**(3), p 475-492
11. M. Gaune-Escard, L. Rycerz, W. Szczepaniak, and A. Bogacz, Enthalpies of Phase Transition of the Lanthanide Chlorides $LaCl_3$, $CeCl_3$, $PrCl_3$, $NdCl_3$, $GdCl_3$, $DyCl_3$, $ErCl_3$ and $TmCl_3$, *J. Alloys Comp.*, 1994, **204**, p 193-196
12. D.H. Templeton and G.F. Carter, The Crystal Structures of Yttrium Trichloride and Similar Compounds, *J. Phys. Chem.*, 1954, **58**(11), p 940-944
13. H. Bommer and E. Hohman, The Heats of Solution and Formation of Water-free Chlorides of Rare Earth Metals, *Z. Anorg. Allgem. Chem.*, 1941, **248**(4), p 373-382
14. F. Weigel and V. Wishnewsky, Die Dampfphasenhydrolyse von Lanthaniden(III)-chloriden, 2. Wärmetönung und Gibbs-Energie der Reaktion $DyCl_3(f) + H_2O(g) = DyOCl(f) + 2HCl(g)$ Wärmetönung der Polymorfen Umwandlung $\beta\text{-}DyCl_3 \rightarrow \gamma\text{-}DyCl_3$, *Chem. Ber.*, 1969, **102**(1), p 5-13
15. J. Nölting, Disorder in Solids Ionic Crystals and Metals, *Angew. Chem. Internat. Edit.*, 1970, **9**(7), p 489-500
16. K. Funke, D. Wilmer, T. Lauxtermann, R. Holzgreve, and S.M. Bennington, On the Dynamics of Frenkel Defect Formation and Ionic Hopping in AgCl, AgBr and β-AgI, *Solid State Ionics*, 1996, **86-88**, p 141-146
17. C.S. Sunandana and P. Senthil Kumar, Theoretical Approaches to Superionic Conductivity, *Bull. Mater. Sci.*, 2004, **27**(1), p 1-17
18. L. Rycerz, M. Szymanska, P. Kolodziej, I. Chojnacka, and M. Gaune-Escard, Disorder in Solid AgCl and AgBr, unpublished results